Improving contrast and sectioning power in confocal imaging by third harmonic generation in SiO_x nanocrystallites

Gilbert Boyer and Karsten Plamann

Laboratoire d'Optique Appliquée, École Polytechnique-École Nationale Supérieure de Techniques Avancées-CNRS UMR 7639, Centre de l'Yvette, chemin de la Hunière, 91761 Palaiseau cedex, France

Received November 1, 2006

We present a new optical microscope in which the light transmitted by a sample-scanned transmission confocal microscope is frequency-tripled by SiO_x nanocrystallites in lieu of being transmitted by a confocal pinhole. This imaging technique offers an increased contrast and a high scattered light rejection. It is demonstrated that the contrast close to the Sparrow resolution limit is enhanced and the sectioning power are increased with respect to the linear confocal detection mode. An experimental implementation is presented and compared with the conventional linear confocal mode.

OCIS codes: 180.0180, 180.1790, 110.0110, 110.6880.

Nonlinear laser scanning microscopy allows for considerably increased measuring depths and provides additional imaging modes by the stimulation of frequency doubling and tripling in the sample. Harmonic generation may as well be used in the *detection* branch of a microscope: in a confocal transmission geometry. References [1] and [2] reported the use of a frequency doubling crystal to gate out multiply scattered photons and to provide a so-called virtual pinhole. The present work attempts to further enhance this effect by increasing the order of the harmonic conversion and using optically nonlinear particles of submicron size. Nanometric crystallites have been observed to enhance the electromagnetic field in their vicinity[3], which may lead to bandgap structures, particle plasmon resonances, luminescence effects and the enhancement of bulk nonlinearities[4−7].

We prepared SiO_x nanocrystallites by femtosecond laser ablation of a silicon substrate and redeposition on a standard glass coverslip. The deposition was performed in a 10^{-6} mbar vacuum using 500-μJ laser pulses at a wavelength of 620 nm and a repetition rate of 10 Hz focused into a spot of roughly 100 μm in diameter. The residual oxygen in the cavity resulted in at least partly oxidized particles. The typical distance between crystallites on the substrate varied from about 1 μm to several tens of microns. For the experiments it was verified that only one crystallite contributed to the third harmonic conversion. The crystal or cluster size being about 100 to 150 nm, they could be considered as point-like objects for all optical considerations. Under excitation by femtosecond laser radiation at 1260 nm, strong third harmonic generation (THG) was observed. It was however beyond the scope of the present study to quantify the third order susceptibility or to identify the underlying process (i.e. nonlinearity of the particles or enhancement of surface effects). In our experiments, the particles replace the pinhole in a sample-scanned transmission confocal microscopy setup, as shown in Fig. 1. We use a home built Cr^{4+}:forsterite laser emitting nanojoule pulses with a pulse duration of about $40-50$ fs at a wavelength of 1260 nm and a repetition rate of 84 MHz. The laser is pumped by a diode-pumped Yb:glass fiber laser assuring a good long-term stability. Incidentally, the central wavelength is quite close to the wavelength for which group velocity dispersion changed sign of most of the usual optical elements, so pulse-broadening effects in the optical components are believed to be small and are neglected in the present work[8]. The expanded laser beam is focused onto the sample by a water immersion microscope objective (Olympus UplanApo/IR 60×, numerical aperture (NA) of 1.2 with correction for the coverslip thickness) through a standard coverslip. The transmission of the objective itself may be estimated to be about 60%. Additional losses by overfilling the pupil may be estimated to be about 50%. The sample could be positioned freely in all three dimensions with nanometric precision by a piezoelectric translation stage with capacitive position-sensors (Piezosystem Jena). The light transmitted through the sample travels through an additional coverslip and is collimated by an identical collector (exit pupil ~ 8 mm)[9]. The beam is then focused onto a nanocrystal by a third objective (Olympus UPlanFl 20×, NA = 0.5). It generates frequency-tripled light by THG which is collected by a lens and detected by a photomultiplier tube (PMT) protected by filters from environmental stray light and the fundamental laser wavelength. Optionally, the photo-

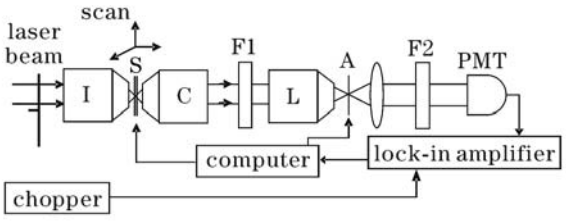

Fig. 1. Diagram of the experiment. I: illumination objective (60×, NA = 1.2); C: collection objective (same type as I); S: sample on a three-dimensional scanning stage; F1: RG 1000 Schott glass filter; L: focusing lens (20×, NA = 0.3); A: SiO_x nanocrystal on a coverslip substrate; F2: KG 5 Schott glass filter.

1671-7694/2007/080477-03

multiplier output could be filtered by a lock-in amplifier tuned to the frequency of a beam chopper placed in the path of the laser beam. For comparison, the third objective could be replaced by a 50-mm lens, the nanocrystal by a conventional pinhole, and the photomultiplier by a photodiode sensitive to the fundamental laser wavelength.

Except for the frequency tripling, our setup is equivalent to a detection geometry using a pinhole, it allows for a simpler analysis than the aforementioned virtual point detector[1,2]. The scheme is basically a confocal transmission microscope with a point detector whose output is the third harmonic of the linear signal with additional gating of scattered photons. As the dimensions of the particle are much smaller than the wavelength, their spatial sensitivity distribution may be expressed by a spatial delta function. Consequently, the image formation equation can be written as

$$I_{\mathrm{THGD}}(x,y,z) = \left\{ \left| h_1(x,y,z) \times h_2(x,y,z) \otimes t(x,y,z) \right|^2 \right\}^3, \quad (1)$$

where I_{THGD} is the signal in the THG detection (THGD) mode, h_1 and h_2 are the amplitude point spread functions (PSFs) of the illumination and collection objectives, respectively, and t is the amplitude transmission function of the sample. The cubic exponent accounts for the THG detection process[10−12]. The instrument therefore measures the differential transmission of the object with a response that is cubic in the transmitted intensity and rejects multiply scattered photons. Equation (1) assumes that our imaging mode is coherent; hence the optical bandwidth is not enlarged with respect to the linear confocal microscope. However, it is interesting to examine some specificities arising from the cubic response. We may use Eq. (1) to calculate the resolution limit of the THGD microscope according to the Sparrow criterion for coherent imaging which states that for a two-point object defined by

$$t(v) = \delta(v+a) + \delta(v-a), \quad (2)$$

the points are separated when the image intensity is constant as we move from one image point to the other in the image plane[13]. Figure 2 shows the comparison between the calculated image profiles which would be obtained from a confocal microscope for a separation distance corresponding to the Sparrow limit and for a distance 20% above the Sparrow limit. The image profiles for the same objects calculated for the THGD mode are also shown in Fig. 2. The separation between the points at 1.2 times the Sparrow limit is considerably more pronounced in the THG image. While the THGD mode does not actually lower the Sparrow resolution limit — a plateau in linear confocal mode remains a plateau in THGD mode — it enhances image contrast for object details close to that limit.

A similar reasoning may be applied to the sectioning power. To quantify the sectioning power, it is useful to examine the variation of the integrated intensity for a point object defined as[9]

$$I^{\mathrm{int}}_{\mathrm{THGD}}(u) = 2\pi \int_0^{\infty} I_{\mathrm{THGD}}(u,v) v \mathrm{d}v, \quad (3)$$

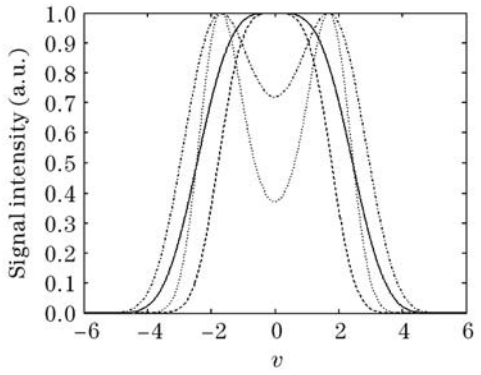

Fig. 2. Computer calculated profiles of images of a two-point object. The curves are obtained at a distance corresponding to the Sparrow resolution criterion as observed by a confocal microscope (solid line), at the same distance as observed in THG mode (dashed line), two-point image separated by 1.2 times the Sparrow limit in confocal (dash-dot) and THG observation mode (dashed line).

where u is the axial coordinate in optical units and v is the radial coordinate with respect to the optical axis. The half-width of this function indicates how the instrument discriminates against out-of-focus planes in the object: when moving away from the focal plane the integrated intensity decays rapidly, reaching the half power at $u = 2.33$, different from the value $u = 4.27$ calculated for a linear confocal microscope. Furthermore, secondary axial lobes are suppressed, which in the case of superresolution approaches by Fourier plane filtering would relax the constraints and expand the possibilities (see, for instance, chapter 6 in Ref. [9]).

For the experimental verification of the above considerations it is first demonstrated that the nonlinear process actually corresponds to THG. The imaging properties in terms of lateral and axial resolution are then compared with the linear confocal mode.

To characterize the harmonic light emitted by the nanoparticles under femtsosecond laser excitation, the substrate covered with nanoparticles was placed at the sample position in Fig. 1. THG radiation was collimated by the collector objective towards the focusing lens of an optical fiber coupled with a Thorlabs SP1 spectrometer of 3 nm in resolution, or a PMT (Hamamatsu R636) whose As-Ga photocathode was insensitive to pump radiation. Intensity variations between individual microcrystals remained within one order of magnitude. The average pump power was measured before the objective lens across a diaphragm having the same diameter as the entrance stop of the objective. The spectrum of the harmonic radiation emitted by the nanocrystals layer shows a strong band located at 417 nm. The weak broadband spectrum corresponds to residual background noise, indicating that the up-converted frequency is due to a THG process but not fluorescence. This is confirmed by the cubic dependence of THG on average pump power. The particle THG could be estimated to be about three orders of magnitude stronger than the one measured on the substrate alone.

To evaluate the possible influence of the size of nanoparticles, we have scanned the nanocrystal layer laterally and axially across the focus diffraction pattern

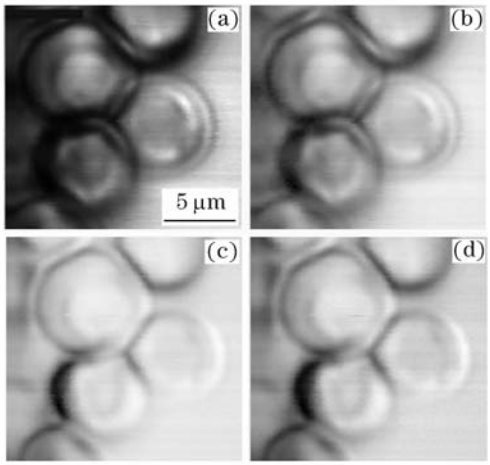

Fig. 3. Microscopic images of Dawsonia superba spores (a) in the THGD mode and (b) the corresponding cube-root version, (c) in the linear confocal mode and (d) the corresponding cube version. Average input power is 24 mW at the back pupil of the objective. The gray scale is linear from zero (black) to the maximum signal of each individual image (white).

of the beam. A full-width at half-maximum (FWHM) of 380 nm was observed which is of a deviation within 3% to the value of 370 nm calculated from the diffraction-limited PSF by taking into account the cubic dependence. Axially, the extension of the theoretical (cubic) PSF is 910 nm whereas the experiment yields 1.09 μm. This small discrepancy to theory may in fact be explained by some residual aberration of the objective, resulting in a slightly lower-than-nominal effective NA[14]. Still, these results validate the aforementioned analysis of the imaging process.

In the following we describe the experiments performed with the full setup of Fig. 1, either in THG detection mode or by making linear confocal microscope images of the same sample. The confocal scanning optical microscope (CSOM) version was made by substituting an achromatic doublet 50 mm in focal length to the 20× focusing objective lens and by positioning a pinhole 3 μm in diameter in front of a near infrared (NIR) photodiode (Thorlabs DET410) that was substituted to the PMT. The detector normalized radius was then 0.54[15]. The maximum average power was 24 mW at the back pupil of the illumination objective. The specimen was spores of Dawsonia superba. Images were individually normalized and had the same number of pixels (200 × 200). The THGD mode displayed in Fig. 3(a) shows high contrast and is rich in detail, which may be attributed to the higher sectioning power and the suppression of scattered light. The cubic root of the same data is shown in Fig. 3(b) to allow a direct comparison with the linear detection image (Fig. 3(c)) which shows less contrast and details. The data of linear detection raised to the power of three are shown in Fig. 3(d) for comparison with the THGD mode. Despite the artificially enhanced contrast, the result is of lower quality than in the THGD mode and the noise is increased in comparison with its linear counterpart.

In conclusion, we have demonstrated a novel nonlinear imaging mode for CSOM that takes advantage of the newly discovered properties of silicon-oxide nanocrystals and clusters of nanocrystals generating strong THG signals. No harmonic generation is stimulated *within* the sample and therefore no risk of photodamaging the sample by short wavelength light exists. This mode delivers the cube-intensity image and it suppresses non-ballistic photons by the intrinsic time-gating of the detection. It enhances contrast on samples having weak differential absorption and it delivers slightly improved resolution because it replaces the confocal pinhole by a point-like detector. The increase in contrast and sectioning power is obtained without actually increasing the spatial frequency bandwidth and may therefore be considered as *relaxed superresolution*, following an argument by Wilson *et al.*[9]. In contrast to superresolution by pupil filtering, this increase is not submitted to the classical trade-off resolution-luminosity-side lobes, but can support superresolving lenses, owing to the very low level of the side lobes.

The SiO_x nanocrystals and clusters were deposited by D. Scuderi, O. Albert, A. Dos Santos and J. Etcheparе at the LOA. We thank Bertrand Reynier, Unité de Mécanique, ENSTA, France, for sample characterization by electron microscopy. K. Plamann is the author to whom the correspondence should be addressed, his e-mail address is karsten.plamann@ensta.fr.

References

1. C. Yang and J. Mertz, Opt. Lett. **28,** 224 (2002).
2. T. Pons and J. Mertz, J. Opt. Soc. Am. B **21,** 1486 (2004).
3. M. Quinten, Appl. Phys. B **73,** 245 (2001).
4. C. Wu, C. H. Crouch, L. Zhao, and E. Mazur, Appl. Phys. Lett. **81,** 1999 (2002).
5. S. Amuroso, R. Bruzzese, N. Spinelli, R. Velotta, M. Vitiello, X. Wang, G. Ausanio, V. Iannotti, and L. Lanotte, Appl. Phys. Lett. **84,** 4502 (2004).
6. L. A. Golovan, L. P. Kuznetskova, A. B. Fedotov, S. O. Konorov, D. A. Sidorov-Biryukov, V. Y. Timoshenko, A. M. Zheltikov, and P. K. Kashkarov, Appl. Phys. B **76,** 429 (2003).
7. S. O. Konorov, A. B. Fedotov, A. A. Ivanov, M. V. Alfimov, S. V. Zabotnov, A. N. Naumov, D. A. Sidorov-Biryukov, A. A. Podshivalov, A. N. Petrov, L. Fornarini, M. Carpanese, G. Ferrante, R. Fantoni, and A. M. Zheltikov, Opt. Commun. **224,** 309 (2003).
8. G. Agrawal, *Nonlinear Fiber Optics* (Academic Press, New York, 2002).
9. T. Wilson and C. J. R. Sheppard, *Theory and Practice of Scanning Optical Microscopy* (Academic Press, London, 1984).
10. Y. Barad, H. Eisenberg, M. Horowitz, and Y. Silberberg, Appl. Phys. Lett. **70,** 922 (1997).
11. J. A. Squier, M. Müller, G. J. Brakenhoff, and K. Wilson, Opt. Express **3,** 315 (1998).
12. J. M. Schins, Schrama, J. Squier, G. J. Brakenhoff, and M. Muller, J. Opt. Soc. Am. B **19,** 1627 (2002).
13. R. Guenther, *Modern Optics* (John Wiley & Sons, New York, 1990).
14. R. Juškaitis, "Characterizing high numerical apertures microscope objective lenses" in *Optical Imaging and Microscopy, Springer Series in Optical Sciences* Török and Kao, (eds.) Vol. 87 (Springer-Verlag, Berlin, 2003).
15. M. Gu, *Principles of Three-Dimensional Imaging in Confocal Microscopes* (World Scientific, Singapore, 1996).